Science Bulletin 63 (2018) 300–305

Contents lists available at ScienceDirect

Science Bulletin

journal homepage: www.elsevier.com/locate/scib

Science Bulletin
www.scibull.com

Article

# Application of microprobe-based flank method analysis of $Fe^{3+}$ in garnet of North Qilian eclogite and its geological implication

Xiaoli Li [a,*], Shuguang Song [a], Lifei Zhang [a], E. Heidi Höfer [b]

[a] The Key Laboratory of Orogenic Belts and Crustal Evolution MOE, School of Earth and Space Sciences, Peking University, Beijing 100871, China
[b] Institut für Geowissenschaften, Facheinheit Mineralogie, Johann Wolfgang Goethe-Universität, D-60054, Germany

ARTICLE INFO

*Article history:*
Received 9 November 2017
Received in revised form 21 January 2018
Accepted 25 January 2018
Available online 6 February 2018

*Keywords:*
Microprobe
Flank method
Ferric iron
Garnet
North Qilian eclogite

ABSTRACT

A newly developed microprobe-based methodology (the Flank Method) for $Fe^{3+}/\Sigma Fe$ quantification has been successfully applied to some natural garnets from the North Qilian eclogites by JEOL JXA-8100 microprobe at Peking University. The results demonstrated an obvious discrepancy in comparison with the outcomes by conventional stoichiometric calculations. This methodology allows to measure the $Fe^{3+}/\Sigma Fe$ ratio and perform elemental analyses simultaneously in the same condition. Accurate in-situ measurement of $Fe^{3+}$ content in garnet may bring certain impact on the garnet-based P-T estimation. According to the compositional zonation displayed in the studied eclogitic garnets from North Qilian, a prograde metamorphic *PT* path from 19.5 kbar, 520 °C to 22 kbar, 600 °C was reconstructed. More interestingly, the measured $Fe^{3+}/\Sigma Fe$ ratios in garnets decreasing from core to rim may probably imply that the oxygen fugacity ($fO_2$) declines with the depth of the subduction zone.



## 1. Introduction

Garnet is an important Fe-bearing mineral in metamorphic rocks. Its compositional zonation that may reveal important geological information (e.g. P-T conditions, oxygen fugacity etc.) [1,2]. The ferric iron content in garnet is commonly estimated by indirect methods, such as stoichiometric recalculation from microprobe elemental analyses. However, due to inherent analytical precision, the arising uncertainty of $Fe^{3+}/\Sigma Fe$ determination in garnet will lead to further questions about the related P-T estimation and redox-state evaluation [3–7]. A recently developed microprobe-based (*in-situ*) methodology termed as the Flank Method [8] has been successfully applied to natural garnets for $Fe^{3+}/\Sigma Fe$ determination with very satisfied outcomes [9]. It is a hybrid method measuring both the iron's Lβ/Lα intensity ratios and peak shifts that thus has "dramatically" enhanced the analytical sensitivity, particularly comparing to the early attempts [10–12]. In comparison with other direct analytical methods, such as Mössbauer spectroscopy, XANES (X-ray absorption near edge structure) and XAFS (X-ray absorption fine structure) with synchrotron or XPS (X-ray photoelectron spectroscopy) techniques, the microprobe analysis is a non-destructive method, which allows *in-situ* measurement of $Fe^{3+}/\Sigma Fe$ ratios on a micrometer scale without additional sample preparation, and provides simultaneous analyses of major (and trace) element chemistry on the same spot in the same condition. These very advantages of this methodology offer the possibility to perform *in-situ* accurate determination of ferric and ferrous iron contents in garnet (and other minerals), which is of particular importance in the P-T calculation by using Fe-Mg exchange geothermobarometry or (bulk) phase equilibria modeling. Also, the oxidation state of iron in garnet plays a key role in the evaluation of the redox state and oxygen fugacity of garnet-bearing rocks from subduction zones and cratonic lithosphere [13,14].

In this study, we succeeded in applying this methodology on the JEOL JXA-8100 microprobe at Peking University to several natural garnets from the North Qilian eclogites, which are typical high-pressure low-temperature metamorphic rocks in oceanic-type subduction zone [15]. By re-evaluating the ferrous content in garnets using direct flank method microprobe analyses, we re-estimated the possible impact on the metamorphic *PT* path of North Qilian eclogites and proposed a likely associated oxygen-activity change pattern during subduction process.

## 2. Flank method analyses

The principle for the microprobe $Fe^{3+}/\Sigma Fe$ quantification is based on the soft FeL X-ray emission shift phenomenon: there is a distinct peak shift of FeLα and FeLβ spectra lines to lower energies with increasing $Fe^{3+}$, as well as a noticeable change in the

* Corresponding author.
*E-mail address:* xiaoli.li@pku.edu.cn (X. Li).

https://doi.org/10.1016/j.scib.2018.01.025
2095-9273/

intensity (counts) ratio with the iron's oxidation state (Fig. 1a,b). The flank method considers both peak shifts and relative intensities (peak area) effects: it measures the intensity ratio of iron's peak flanks (cpsLβ/cpsLα) – those flank positions of both FeLα and FeLβ emission lines, where the spectra differences of $Fe^{2+}$- and $Fe^{3+}$-bearing samples (such as almandine and andradite) are most pronounced [8,16] (Fig. 1a-b, FeLα*, FeLβ*). The flank method measurement positions are mainly determined by the absorption spectra, which are defined by two factors: (1) accelerating voltage (electron penetration depth) and (2) total Fe concentration in the sample. Höfer and Brey [9] have experimentally determined the optimal accelerating voltage at 15 kV that happens to be consistent with the condition in conventional microprobe elemental analyses. The total Fe abundance has a significant impact on the iron's Lβ/Lα ratio due to self-absorption effect, which commonly requires relevant corrections (ZAF, PRZ etc.); while the Lβ/Lα ratio is mainly governed by the (linear) absorption effect caused by $Fe^{2+}$ [8,9], thus, it can be utilized to quantify the $Fe^{3+}/\Sigma Fe$ in the sample. For garnets, the Lβ/Lα–$Fe^{2+}$ dependency changes with both $Fe^{3+}$ and ΣFe variations that can be expressed by multiple linear regression function (see Eq. (3), Figs. 11 and 13 in [9]). As a result, with accurate ΣFe determination, exact $Fe^{2+}$ content (in garnet) can be

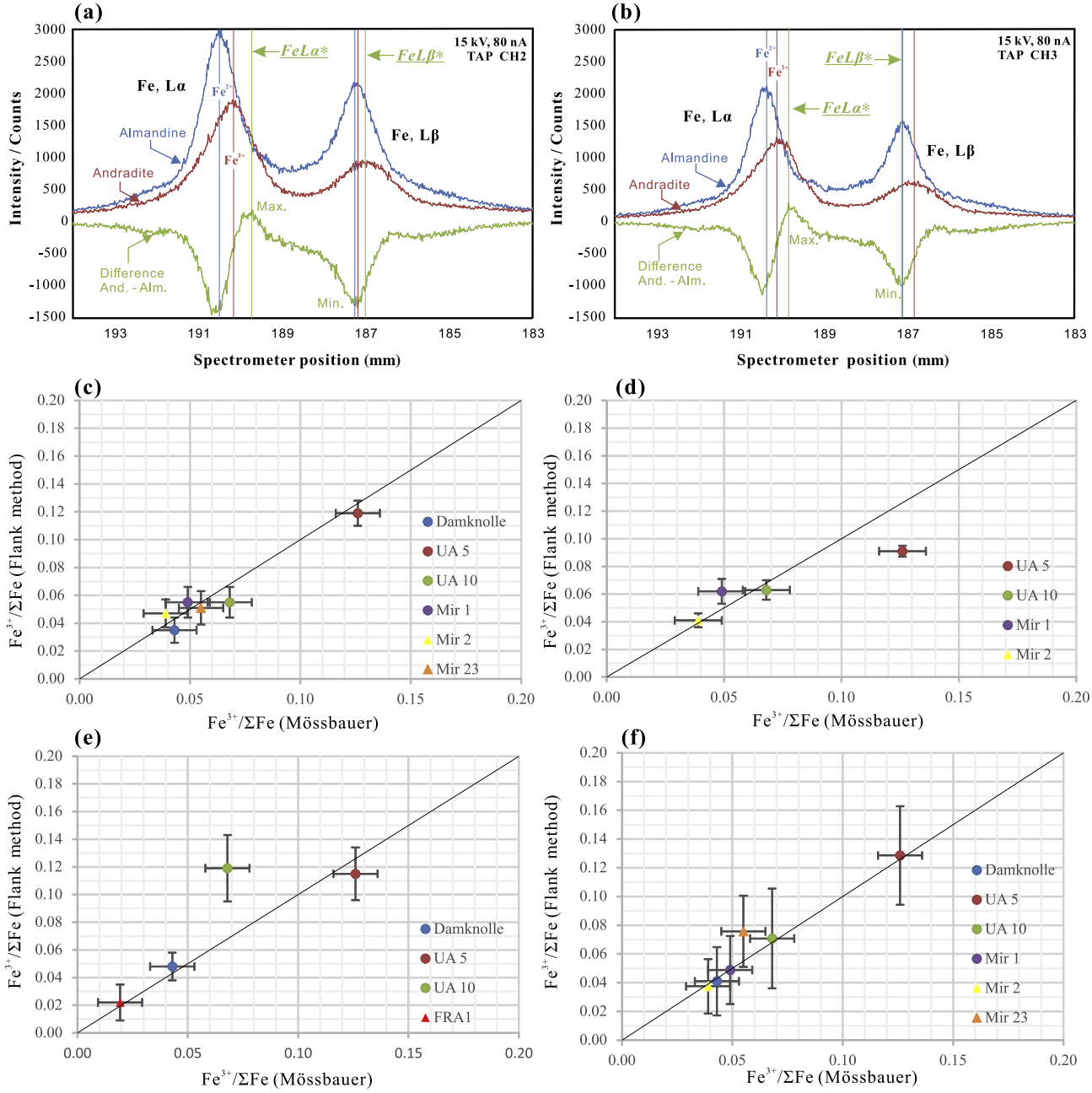


**Fig. 1.** (a-b) The spectra of FeL X-ray emission lines of $Fe^{2+}$-bearing garnet (standard almandine Alm_oxy from McGuire et al. [18], in blue), $Fe^{3+}$-bearing garnet (standard andradite-skiagite from Woodland and Ross [19], in red), and their difference spectrum (And.-Alm., in green), obtained by two TAP-spectrometers of (a) CH2 and (b) CH3 of JEOL JXA-8100 microprobe (15 kV, 80 nA) at Peking University; the flank method measuring positions (FeLα* and FeLβ*) are defined where the differences are most pronounced. (c–f) The measured $Fe^{3+}/\Sigma Fe$ ratios results of standard garnets by flank method (this work, error bars 1σ = 0.01–0.02), in comparison with their Mössbauer data (from relevant literatures [20–22], error bars 1σ = 0.01).

acquired by measuring the iron's Lβ/Lα ratio and using standard garnets of known $Fe^{3+}/\Sigma Fe$ ratios for calibration (an Excel spreadsheet is available for this).

In this study, the flank method analyses were carried out on the JEOL JXA-8100 microprobe equipped with four wavelength dispersive spectrometers (WDS) at Peking University. There are two TAP diffraction crystals were installed on two separate spectrometers (CH2, CH3) of our JXA-8100 microprobe that can be used for FeL emission line measurement. Comparatively the TAP crystal in spectrometer CH2 demonstrated a better resolution (Fig. 1a-b) and was furtherly used in the flank method analysis, while the spectrometer CH3 was assigned for Na, Al, Si, Mg analyses. First and foremost, routine elemental (quantitative) analyses for garnets should be performed beforehand to ensure that proper standards were selected correctly, and then perform the flank method measurement. The routine microprobe analyses for oxides were after Li et al. [17] in the condition of 15 kV, 10 nA and SPI 53 mineral standards (U.S.) were utilized.

The high precision of flank method analysis is principally defined by the accuracy of the spectrometer position and its reproducibility, especially for the JEOL series microprobe with motor-driven spectrometers. A sophisticated spectrometer calibration procedure was conceived by Höfer and Brey [9], via peak search for the sharp iron's 9th order Kα (FeKα9th) peak position; it should be carried out in advance for each working session (in this work, 24 h was recommended). To enhance the statistical precision, accumulation analyses (5 × 5 grid, 2 μm step, total 25 spots for 1 group of effective analyses) were utilized in this work, which indeed had reduced the relative error in $Fe^{3+}/\Sigma Fe$ determination to $1\sigma = \pm 0.01$ ($N < 100$); however, this approach resulted in a long analytical time for 1 effective outcome to approximate 130 min (5 min for each spot), that only a few effective analyses could be accomplished in one work session.

Standard garnets with known $Fe^{3+}/\Sigma Fe$ values (Mössbauer data by other researchers) of Alm_oxy [18], andradite-skiagite [19], FRA1 (32.26 wt% ΣFe, 0.62 wt% $Fe^{3+}$) [20], Damknolle (15.18 wt% ΣFe, 0.77 wt% $Fe^{3+}$), Mir1 (8.60 wt% ΣFe, 0.42 wt% $Fe^{3+}$), Mir2 (10.04 wt% ΣFe, 0.39 wt% $Fe^{3+}$), Mir13 (10.66 wt% ΣFe, 0.53 wtm % $Fe^{3+}$), Mir23 (8.31 wt% ΣFe, 0.46 wt% $Fe^{3+}$) [21] and UA5 (6.49 wt% ΣFe, 0.82 wt% $Fe^{3+}$), UA10 (6.23 wt% ΣFe, 0.42 wt% $Fe^{3+}$) [22] were used for the analytical condition examination and further calibration of measured samples. Four (or more) standard garnets were analyzed firstly, and then the unknown samples. Detailed descriptions of spectrometer calibration and flank method measurement procedures are summarized in Appendix 1.

## 3. Results

The studied samples were collected from the Baijingsi cross-section, about 30–40 km to the east of Qilian Town; they are all epidote-eclogite type, and include (A) massive (sample Q05-1) and (B) foliated ones (samples 2Q19-3 and 08BSY-38) due to their field appearance (see in [23]). Their detailed studies of petrology, mineralogy and metamorphic P-T conditions have been well described in the literatures [15,23,24].

The garnets from both massive and foliated eclogite samples are mostly of ideal idiomorphic crystals with considerable sizes (~2–5 mm) (Fig. 2). The garnets from the massive sample (Q05-1) usually contain a few mineral inclusions as rutile, epidote, calcite, quartz, plagioclase and iron sulphide ($FeS_x$) (Fig. 2a, b); while the garnets from the foliated samples (2Q19-3 and 08BSY-38) often contain numerous inclusions of quartz, rutile, epidote and casually iron oxide ($FeO_x$), displaying certain orientations (foliations) as the matrix minerals (see in [23]) (Fig. 2c, d).

In the flank method measurement, the standard garnets were firstly analyzed; they all yielded consistent results with their

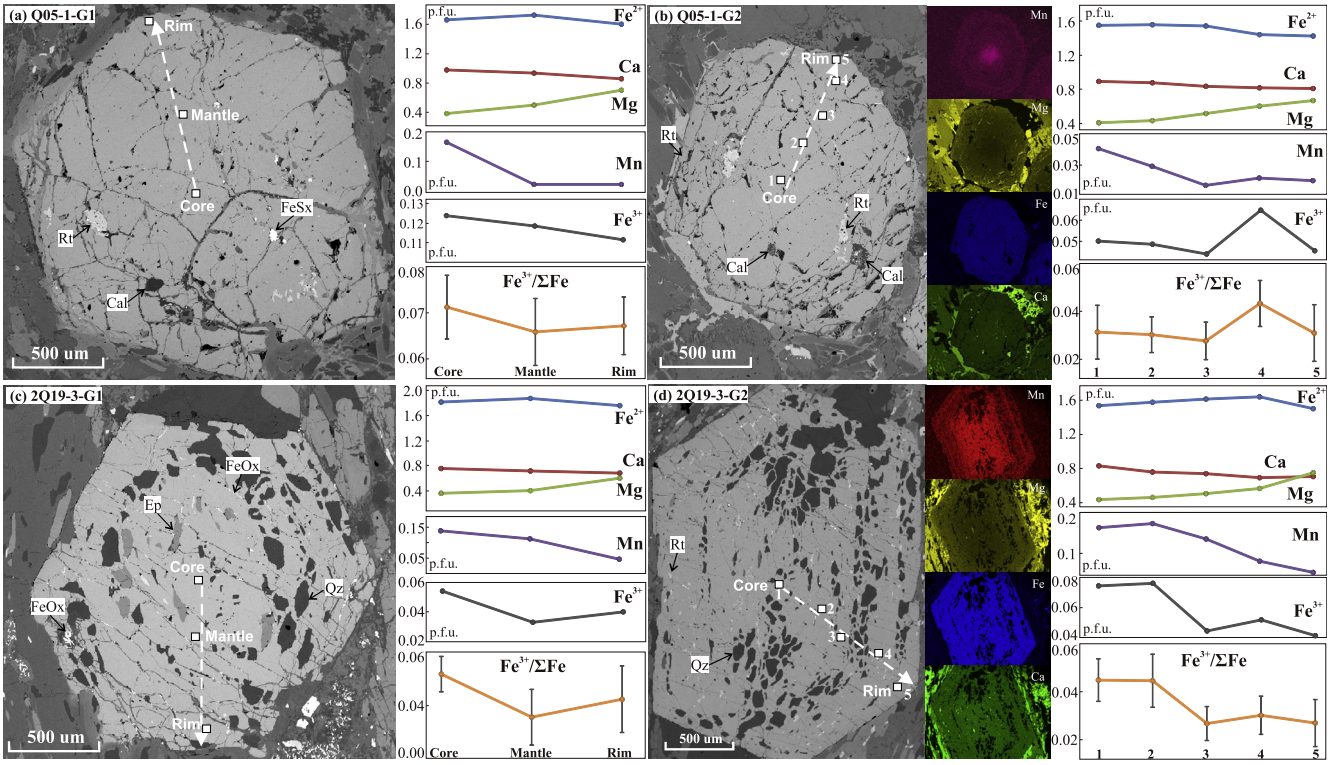


**Fig. 2.** The BSE images and relevant EDS elemental mapping results of the studied garnets from North Qilian massive (a-b: sample Q05-1, garnets G1 and G2) and foliated (c-d: sample 2Q19-3, garnets G1 and G2) eclogites (inclusion minerals Rt – rutile, Cal – calcite, FeSx – iron sulphide, FeOx – iron oxide, Qz – quartz and Ep – epidote). The flank method microprobe analyses results of Ca, Mg, Mn, $Fe^{2+}$, $Fe^{3+}$ contents (in p.f.u.) and $Fe^{3+}/\Sigma Fe$ ratios (error bar $1\sigma$) from core to rim (1 → 2→3 → 4 → 5) are presented aside.

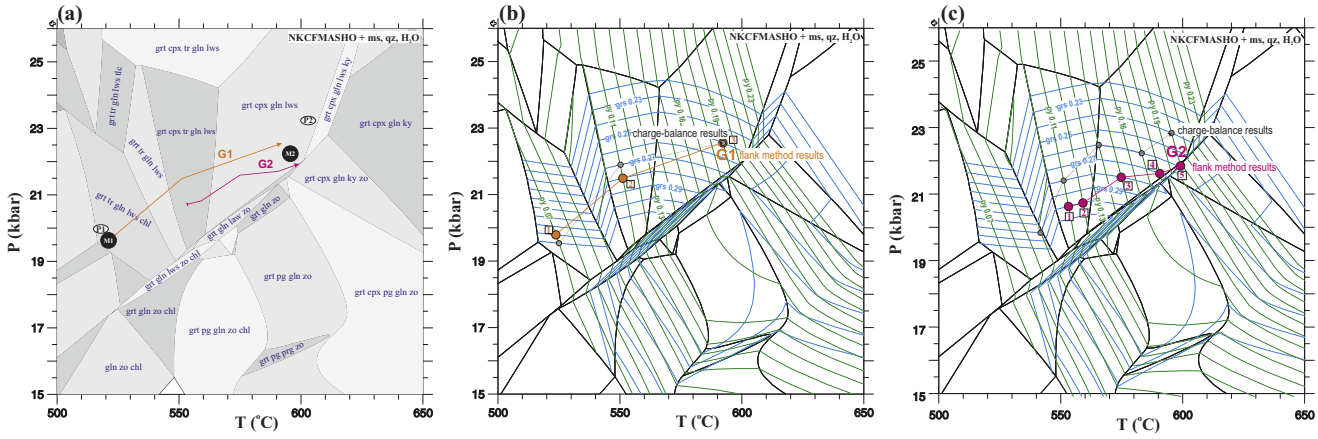


**Fig. 3.** Phase equilibria modelling results (NKCFMASHO) of the massive eclogite sample Q05-1 from North Qilian: (a) pseudosection with inferred P-T paths (M1 → M2 in this work, P1 and P2 from Wei et al. [24]) based on the compositions of garnets G1 and G2; (b-c) the P-T vectors inferred from the compositions of garnet G1 and G2, which were estimated by charge-balance method (grey circles, dotted lines with arrow) and flank method measurement (filled circles, solid lines with arrow) separately.

Mössbauer data in general (Fig. 1c-d). It ensured our measurement's accuracy and allowed further analyses on the eclogitic samples. In results, the studied garnets from North Qilian eclogites all yielded certain $Fe^{3+}$ abundance in a range of 1.00–2.00 wt% ($Fe_2O_3$) (Table S1). Although, in the alternative charge-balance method recalculation (O = 12), the $Fe^{3+}$ was barely calculated therein ($Fe^{3+}$ in p.f.u. = 0.00–0.04 or $Fe_2O_3$ 0.0–0.5 wt%) (Table S1). All analyzed garnets from North Qilian eclogites displayed a clear prograde zonation as being previously reported [23,24]: decrease of Ca and Mn with increase of Mg from core to rim. The directly measured $Fe^{3+}$ ($Fe^{3+}/\Sigma Fe$) component also displayed a gentle decline zonation in general (Fig. 2).

To calculate the P-T conditions, we carried out phase equilibria modeling for the massive eclogite sample Q05-1 by Theriak-Domino software with dataset file *tcdb55* (adopted from the Thermocalc database tcds55.txt by Holland and Powell [25]). Relevant mineral solution models in the dataset were the same as those in Li et al. [17]. The NKCFMASHO model system was considered for the modeling and the bulk composition used for modeling was from Cao et al. [23]. The obtained pseudosection (Fig. 3a) was quite similar to the one in the previous report [24]. The compositions of garnets, obtained by both direct flank method analyses and indirect charge-balance recalculation, were all plotted in the pseudosection that yielded different P-T vectors (Fig. 3b-c, G1 and G2). Using the flank method results, we reconstructed a more accurate prograde P-T path from 19.5 kbar, 520 °C (prograde stage M1) to 22 kbar, 600 °C (peak stage M2). As a result, it seems that when the ferric iron content in garnet is not very high, for instance, 1–2 wt% $Fe_2O_3$, the P-T calculation error caused by different ways of $Fe^{3+}$ estimation may somehow be in a tolerable range ($\Delta P < 2$ kbar, $\Delta T < 10$ °C), otherwise, significant error could occur [3]. Nevertheless, we still recommend to perform preliminary analyses on the ferric iron content in garnet in advance for a better and reliable P-T estimation.

Apart from the correct $Fe^{3+}$ determination, the zonation pattern of measured $Fe^{3+}$ ($Fe^{3+}/\Sigma Fe$ ratio) in garnets could be significantly informative for the relationship between the inferred prograde P-T path and a possible change of the oxidation-redox state during oceanic subduction, if considering the $Fe^{3+}$ component as an oxidized agent. Most of the results showed that, the oxidized agent $Fe^{3+}$ in garnet seemed to decrease from core to rim, i.e. along the prograde metamorphic *PT* path; that is to say, it could suggest a likely oxidation decline during metamorphism in the oceanic subduction zone. However, there are also other essential factors such as pressure, temperature, and probably bulk rock composition need to be taken into account, when it comes to the discussion of redox state of lithospheric rocks [13]; thus, further comprehensive and complex investigations are still required. Meanwhile the fluid activity may furthermore yield an oxidation or reduction environment (at least very locally) at certain tectono-metamorphic stage. Examples can refer to the formation of barite and sulphide in Dabie-Sulu UHP eclogite (continental subduction) [26], or the occurrence of graphite and hydrocarbon-fluid in Western Tianshan UHP belt (oceanic subduction) [27], where relevant fluid involvements were accounted for the (local) redox-state change. In this work, iron sulphide ($FeS_x$, sample Q05-1-G1, Fig. 2a) and iron oxide ($FeO_x$, sample 2Q19-3-G1, Fig. 2c) inclusions in the analyzed garnets were noticed that may help to explain the observed zonal curves.

## 4. Conclusions

The microprobe-based flank method measurement is a convenient and accurate analytical approach for $Fe^{3+}/\Sigma Fe$ quantification in garnet, comparing to other alternative techniques of destructive nature. In this work, we have demonstrated the unreliability of conventional stoichiometric calculation for $Fe^{3+}$ determination in garnet widely used in geosciences, which could subsequently affect a correct P-T estimation based on garnet's composition. More importantly, this in-situ methodology can be applied in the discussion on the redox state of garnet-bearing lithospheric rocks by measuring $Fe^{3+}$. In principle, the flank method is also potentially applicable to other important Fe-bearing minerals (such as clinopyroxene, see Vasilyev [22]) for in-situ ferric iron measurement, once appropriate standard(s) will be available.

## Conflict of interest

The authors declare that they have no conflict of interest.

## Acknowledgments

We sincerely thank Senior engineer Dr. Guiming Shu (Peking University) for his assistance in the technical support. This work was financially supported by the National Natural Science Foundation of China (41372060, 41330210 and 41202032).

## Appendix 1

Summary of flank method measurement procedure on JEOL JXA-8100 microprobe is modified after Höfer and Brey [9]. All mentioned Excel spreadsheets are available from the authors for free.

### Appendix 1A. Spectrometer calibration

(1A-1) Utilize the TAP spectrometer(s) to measure the defined cpsLβ/cpsLα ratio in flank method; adjust the target detector slit to its smallest available value for the best resolution (300 μm for JXA-8100).

(1A-2) Execute peak search for iron's 9th order Kα (FeKα9th) peak position ($fe_0$) on pure Fe metal standard at 25 kV, 80nA; set the analytical condition of the assigned TAP-spectrometer to Integral mode (Int.) with optimal PHA (SCA) parameters (probe diameter 0–1 μm, step 10–15 μm, dwell 1500–2000 ms, PHA gain 32).

(1A-3) Define the FeKα9th peak position in current work session ($fe_x$) using either (*a*) serial analysis or (*b*) PeakFitH program (it can be obtained from the authors for free). The purpose is to obtain the shift value (θ, external calibration value) in relation to the theoretical FeKα9th peak position (189.417 mm), which can be utilized to adjust the spectrometer for flank method measurement. The procedure is to carry out at least 3 repetitions at 6 spectrometer positions (*N*) of symmetrical distances ($fe_1$ and $fe_2$) around the measured FeKα9th peak maxima ($fe_0$); the recommended 6 measuring positions is 52 μm window value ($N_2 = N_1 + 52$, $N_3 = N_2 + 52$, …, $N_6 = N_5 + 52$) and 14 μm shift ($fe_1 = fe_0 - 14$, $fe_2 = fe_0 + 14$).

(1A-4) Transfer the obtained results from above (peak intensities/counts, probe current values) into an Excel spreadsheet: plot the 3 values of $fe_1/fe_2$ (current-normalized ratio) *vs.* spectrometer positions to calculate the corresponding regression line and the spectrometer shift (Δ) for $fe_1/fe_2$ in current work session; use this spectrometer shift value to calibrate the FeKα9th peak position ($fe_x = fe_0 + \Delta$), then we will have the shift value as an external calibration $\theta = 189.417 - fe_x$.

(1A-5) Using the external calibration value $\theta$ to define the FeLα and FeLβ positions in flank method measurement. To be noted, this value (i.e. $fe_1/fe_2$) is very specific for each spectrometer and particular JEOL microprobe during this very work session period; it should be maintained as an internal reference and energy calibration for all flank method measurements.

### Appendix 1B. Flank method measurement

(1B-1) After the spectrometer calibration, set up a new quantitative analysis condition file for garnet, in which, the calibrated TAP-spectrometer must be untouched for measuring the iron's cpsLβ/cpsLα ratio ONLY during the whole work session.

(1B-2) Add two fake elements of As and Br to represent FeLα and FeLβ in the ready (calibrated) TAP-spectrometer analytical condition list; and set the fake "peak" measurement positions of As (FeLα) and Br (FeLβ) from the spectrometer calibration procedure. It is recommended to allow long measuring times of 200–300 s, set no background measurement (or default minimum value), differential PHA/SCA mode, and narrow energy window to avoid overlaps with higher-order X-ray emission lines. Example of flank method measurement conditions for all spectrometers (CH1–CH4, JXA-8100) is shown below (Table 1A).

(1B-3) Accumulation analyses (e.g. grid analysis) are recommended to enhance the statistical precision; also, you may increase the number of measurements to increase the counting statistics. To avoid possible contamination artifacts, measure Br (FeLβ) first and then As (FeLα). It is recommended to carry out preliminary conditional analyses without the calibrated TAP-spectrometer, to ensure suitable standard data are selected for all elements. In this work, we used 15 kV, 10 nA analytical condition and SPI 53 minerals (U.S.) standards; although higher beam current of 60–200 nA is also recommended, it requires a perfect vacuum state to maintain such high energy more than 24 h.

(1B-4) Measure four or more standard garnets with known $Fe^{3+}/\Sigma Fe$ values firstly, and then the unknown samples. After the measurement, for routine quantitative elemental determination, run an off-line matrix correction by deleting the two "fake" elements of As and Br, then export the summary data of oxide wt% and atom% (normalized by 12-oxygen); for flank method ratio, export the summary data of the net intensities and beam current values of As and Br. Finally, insert these data into an Excel spreadsheet to calculate the flank method ratios and furtherly $Fe^{3+}/\Sigma Fe$ quantification. To be noted, the weather condition and room temperature may have unpredictable influences on the measurement.

## Appendix 2. Supplementary data

Supplementary data associated with this article can be found, in the online version, at https://doi.org/10.1016/j.scib.2018.01.025.

## References

[1] Spear FS. The calculation of metamorphic phase equilibria I: geothermometry and geobarometry. Metamorphic Phase Equilibria and Pressure-Temperature-Time Paths. Mineralogical Society of America: Monograph; 1993, p. 511–545.
[2] Deer WA, Howie RA, Zussman J. Rock-forming minerals. 2nd ed. London: The Geological Society; 1997.
[3] Luth RW, Virgo D, Boyd FR, et al. Ferric iron in mantle derived garnets: implications for thermobarometry and for the oxidation state of the mantle. Contrib Mineral Petrol 1990;104:56–72.

**Table 1A**
Example of flank method measurement conditions of microprobe JXA-8100 (standards are SPI 53 Minerals).

| Element | Standard | Channel | Crystal | Spect. Pos. (mm) | Back (+) (mm) | Back (−) (mm) | Mes. Time (s) | Bac. Time (s) | PHA/SCA |
|---|---|---|---|---|---|---|---|---|---|
| Mg, Kα | Diopside | CH3 | TAP | 107.407 | 5.000 | 5.000 | 20.0 | 10.0 | Diff |
| Ca, Kα | Diopside | CH1 | PETJ | 107.456 | 5.000 | 5.000 | 20.0 | 10.0 | Int |
| K, Kα | Sanidine | CH1 | PETJ | 119.683 | 5.000 | 5.000 | 10.0 | 5.0 | Int |
| Na, Kα | Jadeite | CH3 | TAP | 129.424 | 5.000 | 5.000 | 20.0 | 10.0 | Diff |
| Al, Kα | Jadeite | CH3 | TAP | 90.517 | 5.000 | 5.000 | 20.0 | 10.0 | Diff |
| Si, Kα | Jadeite | CH3 | TAP | 77.300 | 5.000 | 5.000 | 10.0 | 5.0 | Diff |
| Ti, Kα | Rutile | CH4 | PETJ | 87.985 | 5.000 | 5.000 | 10.0 | 5.0 | Int |
| Fe, Kα | Hematite | CH4 | LIFH | 133.843 | 5.000 | 5.000 | 20.0 | 10.0 | Int |
| Mn, Kα | Rhodonite | CH4 | LIFH | 145.396 | 5.000 | 5.000 | 10.0 | 5.0 | Int |
| Cr, Kα | Cr-oxide | CH4 | LIFH | 158.467 | 5.000 | 5.000 | 10.0 | 5.0 | Int |
| Ni, Kα | Ni-silicide | CH4 | LIFH | 114.478 | 5.000 | 5.000 | 10.0 | 5.0 | Int |
| As, Lα | Fake | CH2 | TAP | 190.537 | 0.000 | 0.000 | 200.0 | 1.0 | Diff |
| Br, Lα | Fake | CH2 | TAP | 189.912 | 0.000 | 0.000 | 200.0 | 1.0 | Diff |

[4] Sobolev VN, McCammon CA, Taylor LA, et al. Precise Mossbauer milliprobe determination of ferric iron in rock-forming minerals and limitations of electron microprobe analysis. Am Mineral 1999;84:78–85.
[5] Dyar MD, Breves EA, Emerson E, et al. Accurate determination of ferric iron in garnets by bulk Mössbauer spectroscopy and synchrotron micro-XANES. Am Mineral 2012;97:1726–40.
[6] Quinn RJ, Valley JW, Page FZ, et al. Accurate determination of ferric iron in garnet. Am Mineral 2016;101:1704–7.
[7] Schingaro E, Lacalamita M, Mesto E, et al. Crystal chemistry and light elements analysis of Ti-rich garnets. Am Mineral 2016;101:371–84.
[8] Höfer HH, Brey GP, Schulz-Dobrick B, et al. The determination of the oxidation state of iron by the electron microprobe. Eur J Mineral 1994;6:407–18.
[9] Höfer HH, Brey GP. The iron oxidation state of garnet by electron microprobe: its determination with the flank method combined with major-element analysis. Am Mineral 2007;92:873–85.
[10] Fischer DW, Baun WL. Band structure and the Titanium LII, III X-ray emission and absorption spectra from pure metal, oxides, nitride, carbide, and boride. J Appl Phys 1968;30:4757–76.
[11] Albee AL, Chodos AA. Semiquantitative electron microprobe determination of $Fe^{2+}/Fe^{3+}$ and $Mn^{2+}/Mn^{3+}$ in oxides and silicates and its application to petrologic problems. Am Mineral 1970;55:491–501.
[12] Tossell JA, Vaughan DJ, Johnson KH. The electronic structure of rutile, wüstite, and hematite from molecular orbital calculations. Am Mineral 1974;59:319–34.
[13] Frost DJ, McCammon CA. The redox state of Earth's mantle. Ann Rev Earth Planet Sci 2008;36:389–420.
[14] Stagno V, Ojwang DO, McCammon CA, et al. The oxidation state of the mantle and the extraction of carbon from Earth's interior. Nature 2013;493:84–8.
[15] Song SG, Zhang LF, Niu Y, et al. Eclogite and carpholite-bearing metasedimentary rocks in the North Qilian suture zone, NW China: implications for Early Palaeozoic cold oceanic subduction and water transport into mantle. J Metamorph Geol 2007;25:547–63.
[16] Höfer HH, Weinbruch S, McCammon CA, et al. Comparison of two electron probe microanalysis techniques to determine ferric iron in synthetic wüstite samples. Eur J Mineral 2000;12:63–71.
[17] Li X, Zhang L, Wei C, et al. Quartz and orthopyroxene exsolution lamellae in clinopyroxene and the metamorphic PT path of Belomorian eclogites. J Metamorph Geol 2018;36:1–22.
[18] McGuire AV, Francis CA, Dyar MD. Mineral standards for microprobe analysis of oxygen. Am Mineral 1992;77:1087–91.
[19] Woodland AB, Ross IICR. A crystallographic and Mössbauer spectroscopy study of $Fe_3^{2+}Al_2Si_3O_{12}$-$Fe_3^{2+}Fe_2^{3+}Si_3O_{12}$, (Almandine-"Skiagite") and $Ca_3Fe_2^{3+}Si_3O_{12}$-$Fe_3^{2+}Fe_2^{3+}Si_3O_{12}$ (Andradite-"Skiagite") garnet solid solutions. Phys Chem Miner 1994;21:117–32.
[20] Woodland AB, Droop G, O'Neill HSTC. Almandine-rich garnet from near Collobrières, southern France, and its petrological significance. Eur J Mineral 1995;7:187–94.
[21] Rankenburg K, Lassiter JC, Brey GP. Origin of megacrysts in volcanic rocks of the Cameroon volcanic chain – constraints on magma genesis and crustal contamination. Contrib Mineral Petrol 2004;147:129–44.
[22] Vasilyev P. The oxidation state of deeply subducted, altered oceanic crust: an experimental study and the evidence from natural samples. PhD thesis. Canberra: The Australian National University; 2016.
[23] Cao Y, Song SG, Niu Y, et al. Variation of mineral composition, fabric and oxygen fugacity from massive to foliated eclogites during exhumation of subducted ocean crust in the North Qilian suture zone, NW China. J Metamorph Geol 2011;29:699–720.
[24] Wei CJ, Yang Y, Su XL, et al. Metamorphic evolution of low-T eclogite from the North Qilian orogen, NW China: evidence from petrology and calculated phase equilibria in the system NCKFMASHO. J Metamorph Geol 2009;27:55–70.
[25] Holland TJB, Powell R. An internally consistent thermodynamic data set for phases of petrological interest. J Metamorph Geol 1998;16:309–43.
[26] Yang H, Zhang LF, Liu FL. Study on barite as an accessory mineral in eclogite from main borehole core of the Chinese Continental Scientific Drilling (CCSD). Acta Petrol Sin 2010;26:2073–82 (in Chinese).
[27] Tao RB, Zhang LF, Liu X. Oxygen fugacity of Earth's mantle and deep carbon cycle in the subduction zone. Acta Petrol Sin 2015;31:1879–90 (in Chinese).